Energy Component Analysis for Dilute Aqueous Solutions of Li^+, Na^+, F^-, and Cl^- Ions

Jayaraman Chandrasekhar,* David C. Spellmeyer, and William L. Jorgensen*

Contribution from the Department of Chemistry, Purdue University, West Lafayette, Indiana 47907. *Received July 12, 1983*

Abstract: Monte Carlo simulations have been carried out on dilute aqueous solutions of Li^+, Na^+, F^-, and Cl^- at 25 °C and 1 atm, using recently developed transferable intermolecular potential functions. The calculated heats of solution, volumes of solution, coordination numbers, and structural results compare favorably with available experimental data. The calculated energies have been partitioned into components representing (i) solute–first solvent shell, (ii) solute–bulk solvent, (iii) first shell–first shell, (iv) first shell–bulk, and (v) bulk–bulk interactions. Comparison of these components with the corresponding results obtained for liquid water provides detailed insight into the nature of solvent reorganization in the different solutions, complementing the structural information provided by hydrogen bonding analyses. The most significant structural consequence is the formation of the first solvation shell, whose solvent molecules exhibit net mutual repulsion. Although the normal hydrogen bonding network of water is established rapidly beyond the first shell, some disruption in the first shell–bulk water interaction is evident, particularly in the Li^+ and Na^+ solutions. In all the solutions, the reorganization associated with the first-shell molecules constitutes the major component of the total solvent reorganization energy. The energetics of the ion and the first solvent shell are also compared with gas-phase results on small ion–water clusters. The degree to which these values follow the trends in total heats of solution is examined.

Fresh insights into the nature of solvation in electrolytic solutions have come in the past decade from gas-phase experiments on ion–molecule clusters.[1,2] The precise thermodynamic data obtained in this way have been complemented by structural characterization of the complexes with use of ab initio quantum mechanical methods.[3,4] The extent to which these results parallel those for dilute solutions is of considerable significance. In particular, it is important to know how well the trends in heats of solution of different ions in a given solvent are reproduced by the corresponding cluster formation enthalpies. Figure 1 compares the difference in the experimental cluster formation enthalpies as a function of the number of water molecules in the cluster for two pairs of ions.[2a,b] The difference in the total heats of solvation[5] for the corresponding ions is also indicated as horizontal lines. While the difference in cluster-formation enthalpies for Na^+ and Li^+ rapidly approaches the infinite limit, this is not so for Na^+ and F^-. In the latter case, even the order of the heats of solution is not reproduced correctly by the cluster enthalpies, which show no sign of converging to the solution value. These are not isolated instances. Thus, the difference in the free energy of formation of acetonitrile clusters of K^+ and Cl^- is nearly identical with the difference in total solvation energies for $n = 4$.[2c] On the other hand, the differential solvation of pyridinium and 4-cyanopyridinium ions is not adequately established by gas-phase results on clusters containing up to 3 water molecules.[2d,6] The reasons for such widely differing behavior are not fully understood. Although intuitive explanations such as cooperative solvent effects have been invoked,[2d] these concepts need confirmation and quantification through modern solution theories.

A related question concerning the ion–solvent clusters is their correspondence in terms of structure and energy to well-defined units like the first and second solvation shells present in solutions. A structural comparison is relatively straightforward since the structures of the clusters can be obtained from ab initio calculations or from empirical ion–molecule potential functions,[3,4] while X-ray and neutron-diffraction methods can be used to characterize structure in solution.[7,8] However, a comparison of the energetics is more complex since experimental solvation energies cannot be directly partitioned into components arising from different solvation shells.

Current theoretical methods which probe liquids at the molecular level are well suited for examining the problems raised above.[9] Monte Carlo and molecular dynamics simulations can be performed now on fairly complex solutions and are capable of providing detailed structural as well as energetic information. Not surprisingly, there have been numerous applications of these techniques, particularly to water and aqueous solutions.[10–18] In

(1) Reviews: Kebarle, P. *Annu. Rev. Phys. Chem.* **1977**, *28*, 445. Franklin, J. L., Ed. "Ion–Molecule Reactions"; Plenum Press: New York, NY, 1972; Vol. 1, Chapter 7, pp 315. Szwarc, M., Ed. "Ions and Ion Pairs"; Wiley-Interscience: New York, NY, 1972; p 27. Conway, B. E.; Bockris, J. O'M., Eds. "Modern Aspects of Electrochemistry"; Plenum Press: New York, NY, 1974; Vol. 9.

(2) (a) Džidič, I.; Kebarle, P. *J. Phys. Chem.* **1970**, *74*, 1466. (b) Arshadi, M.; Yamdagni, R.; Kebarle, P. *Ibid.* **1970**, *74*, 1475. (c) Davidson, W. R.; Kebarle, P. *J. Am. Chem. Soc.* **1976**, *98*, 6125. (d) Davidson, W. R.; Sunner, J.; Kebarle, P. *Ibid.* **1979**, *101*, 1675. (e) Hiraoka, K.; Kebarle, P. *Ibid.* **1977**, *99*, 360. (f) Lau, Y. K.; Saluja, P. P. S.; Kebarle, P. *Ibid.* **1980**, *102*, 7429. (g) Meot-Ner, M. *Ibid.* **1978**, *100*, 4694.

(3) Review: Schuster, P.; Jakubutz, W.; Marius, W. *Top. Curr. Chem.* **1975**, *60*, 1.

(4) (a) Kistenmacher, H.; Popkie, H.; Clementi, E. *J. Chem. Phys.* **1974**, *61*, 799; *Ibid.* **1973**, *59*, 5842; *Ibid.* **1973**, *58*, 1689, 5627. (b) Clementi, E.; Popkie, H. *Ibid.* **1972**, *57*, 1077. (c) Mruzik, M. R.; Abraham, F. F.; Schreiber, D. E. *Ibid.* **1976**, *64*, 481. (d) Briant, C. L.; Burton, J. J. *Ibid.* **1976**, *64*, 2888. (e) Gowda, B. M.; Benson, S. W. *Ibid.* **1983**, *79*, 1235.

(5) Reviews: Bockris, J. O'M.; Reddy, A. K. N. In "Modern Electrochemistry"; Plenum Press: New York, NY, 1970; Vol. 1, Chapter 2, p 45. Desnoyers, J. E.; Jolicoeur, C. In "Modern Aspects of Electrochemistry"; Bockris, J. O'M., Conway, B. E., Ed.; Plenum Press: New York, NY, 1969; Vol. 5, p 1. Rosseinsky, D. R. *Chem. Rev.* **1965**, *65*, 467.

(6) Arnett, E. M.; Chawla, B.; Bell, L.; Taagepera, M.; Hehre, W. J.; Taft, R. W. *J. Am. Chem. Soc.* **1977**, *99*, 5729.

(7) Reviews: Neilson, G. W.; Enderby, J. E. *Annu. Rep. Progr. Chem., Sect. C*, **1979**, *76*, 185. Enderby, J. E.; Neilson, G. W. *Rep. Progr. Phys.* **1981**, *44*, 38. Franks, F., Ed. In "Water. A Comprehensive Treatise"; Plenum Press: New York, NY, 1979; Vol. 6, Chapter 1.

(8) (a) Newsome, J. R.; Neilson, G. W.; Enderby, J. E. *J. Phys. C.: Solid State Phys.* **1980**, *13*, L923. (b) Cummings, S.; Enderby, J. E.; Neilson, G. W.; Newsome, J. R.; Howe, R. A.; Howells, W. S.; Soper, A. K. *Nature (London)* **1980**, *287*, 714.

(9) Lykos, P. G., Ed. "Computer Modelling of Matter"; American Chemical Society: Washington, DC, 1978.

(10) Review: Beveridge, D. L.; Mezei, M.; Mehrotra, P. K.; Marchese, F. T.; Ravi-Shanker, G.; Vasu, T.; Swaminathan, S. In "Advances in Chemistry"; American Chemical Society: Washington, DC, 1983.

(11) (a) Jorgensen, W. L.; Chandrasekhar, J.; Madura, J. D.; Impey, R. W.; Klein, M. L. *J. Chem. Phys.* **1983**, *79*, 926. (b) Jorgensen, W. L. *Ibid.* **1982**, *77*, 4156; *J. Am. Chem. Soc.* **1981**, *103*, 335.

(12) Stillinger, F. H.; Rahman, A. *J. Chem. Phys.* **1974**, *60*, 1545. Swaminathan, S.; Beveridge, D. L. *J. Am. Chem. Soc.* **1977**, *99*, 8392. Berendsen, H. J. C.; Postma, J. P. M.; van Gunsteren, W. F.; Hermans, J. In "Intermolecular Forces"; Pullman, B., Ed.; Reidel Press: Dordrecht, Holland, 1981; p 331. Pangali, C.; Rao, M.; Berne, B. J. *Mol. Phys.* **1980**, *40*, 661.

(13) (a) Jorgensen, W. L. *J. Chem. Phys.* **1981**, *77*, 5757. (b) Jorgensen, W. L.; Madura, J. D. *J. Am. Chem. Soc.* **1983**, *105*, 1407.

0002-7863/84/1506-0903$01.50/0

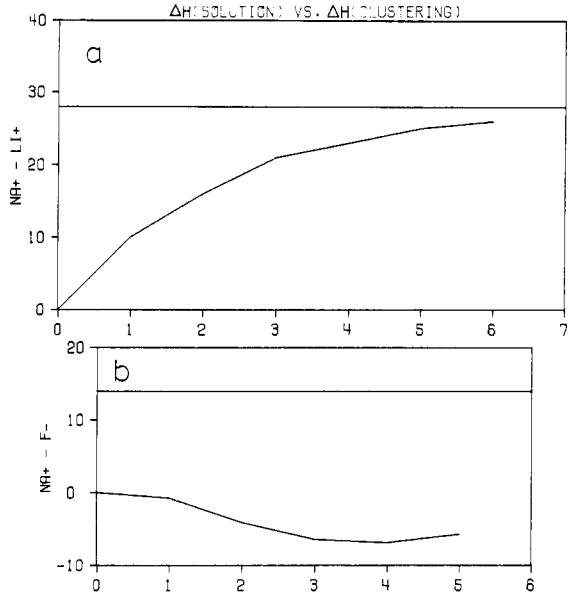

Figure 1. Differences in gas-phase clustering enthalpies (kcal/mol) as a function of cluster size for (a) Na^+ and Li^+ and (b) Na^+ and F^-. The differences in the total heats of solution are shown as horizontal lines.

These studies, the nature of solvation has generally been examined from the structural point of view.[19] Thus, the making or breaking of water structure caused by the solute has been the focus of attention. On the other hand, discussions of the energetic consequences of solvation have generally been limited to the total heat of solution and its two components, the solute–solvent and solvent–solvent energies. In order to obtain a more thorough picture of the energetic changes accompanying solvation, a scheme for the detailed energy component analysis of dilute solutions has been developed as presented here. It involves the identification and computation of the individual contributions to the total solvation energy from the various structural units present in the solution. Such an analysis also provides a framework for relating results for ion–molecule clusters studied in the gas phase to the solvation shells present in solution.

The energy-decomposition procedure has been applied to dilute aqueous solutions of Li^+, Na^+, F^-, and Cl^-. Several simulations using a variety of intermolecular potential functions have been performed previously on these solutions.[15-18] Though reasonable structural results have been obtained, the heats of solution often have been reproduced poorly. Consequently, new ion–water potential functions are reported in the following which yield improved thermodynamic data. They are used in conjunction with the TIP4P potential for water that has been shown to provide structural and thermodynamic results for the pure liquid in good agreement with experiment.[11a] It may also be noted that the present simulations are the first to be performed for these solutions at constant temperature and pressure (25 °C and 1 atm). Extension to higher pressures would be straightforward and could complement the recent diffraction studies of the effects of pressure on the structure of ionic solutions.[20]

Table I. Ion-Water Potential Functions and Interaction Energies

	Li^+	Na^+	F^-	Cl^-
q, e	1.0	1.0	−1.0	−1.0
$A^2 \times 10^{-3}$, kcalÅ^{12}/mol	0.4	14	0.5	26000
C^2, kcalÅ^6/mol	100	300	1200	3500
ΔE (TIPS)[a]	−33.9	−24.1	−24.2	−13.2
ΔE(exptl)[b]	−34	−24	−23.3	−13.1
r_{XO}(TIPS), Å	1.87	2.24	2.49	3.17
r_{XO}(Hartree–Fock)[c]	1.86-1.89	2.22-2.25	2.47-2.51	3.11-3.31

[a] ΔE is the minimum ion-water interaction energy in kcal/mol. [b] Reference 2a,b. [c] Reference 4a.

Computational Details

(a) Potential Functions. The intermolecular interactions are assumed to be pairwise additive. The water monomers are represented by four points, three located on the nuclei and the fourth (M) on the bisector of the HOH angle 0.15 Å from the oxygen toward the hydrogen atoms. The water molecules are rigidly held at the experimental geometry, with r_{OH} = 0.9572 Å and ∠HOH = 104.52°. The interaction between monomers m and n occurs through Coulombic and Lennard-Jones terms involving pairs of sites (eq 1). The charges and the Lennard-Jones parameters for

$$\epsilon_{mn} = \sum_{i}^{\text{on } m} \sum_{j}^{\text{on } n} (e^2 q_i q_j / r_{ij} + A_i A_j / r_{ij}^{12} - C_i C_j / r_{ij}^6) \quad (1)$$

water corresponding to the TIP4P potential are $2q_H = -q_M$ = 1.04, $A_{OO}^2 = 6 \times 10^5$ kcalÅ^{12}/mol and C_{OO}^2 = 610 kcalÅ^6/mol.[11a] This potential represents a slight modification of the TIPS2 function used in earlier investigations on water and aqueous solutions.[11b,13,15] Besides reproducing the experimental density, heat of vaporization, and heat capacity, the TIP4P function yields radial distribution functions and partial structure functions in good agreement with neutron and X-ray diffraction data for liquid water at 25 °C and 1 atm.[11a]

The parameters for the ions were chosen to reproduce the experimental interaction energies and the calculated (Hartree–Fock) geometries of ion–water complexes (Table I). Additional constraints were imposed by requiring the ion–methanol and ion–dimethyl ether (only Li^+ and Na^+ for the latter) interaction energies and geometries to be correctly predicted as well. The reference data were obtained from ab initio calculations with the 6-31G* basis set for the cations[21] and the 3-21+G basis set for the anions.[22] The A and C values for Na^+ differ from the ones used in two earlier studies[15,23] and now appear more consistent with the values expected for an ion of its size. However, the ion–molecule potentials are relatively insensitive to the precise choice of A and C values, since the interaction energies are dominated by the Coulombic term.

(b) Simulations of Dilute Solutions. Monte Carlo simulations were performed on the four dilute solutions, each containing a

(14) (a) Swaminathan, S.; Harrison, S. W.; Beveridge, D. L. *J. Am. Chem. Soc.* **1978**, *100*, 3255, 5705. (b) Mehrotra, P. K.; Beveridge, D. L. *Ibid.* **1980**, *102*, 4287. (c) Owicki, J. C.; Scheraga, H. A. *Ibid.* **1977**, *99*, 7413. (d) Kapaport, D. C.; Scheraga, H. A. *J. Phys. Chem.* **1982**, *86*, 873. (e) Bolis, G.; Clementi, E. *Chem. Phys. Lett.* **1981**, *82*, 147. (f) Bolis, G.; Corongiu, G.; Clementi, E. *Ibid.* **1982**, *86*, 299. (g) Alagona, G.; Tani, A. *Ibid.* **1982**, *87*, 337. (h) Nakanishi, K.; Okazaki, S.; Ikari, K.; Touhara, H. *Ibid.* **1981**, *74*, 428. (i) Okazaki, S.; Nakanishi, K.; Touhara, H.; Watanabe, N. *J. Chem. Phys.* **1981**, *74*, 5863. (j) Geiger, A.; Rahman, A.; Stillinger, F. H. *Ibid.* **1979**, *70*, 263. (k) Pangali, C.; Rao, M.; Berne, B. J. *Ibid.* **1979**, *71*, 2975, 2982. (l) Rao, M.; Berne, B. J. *J. Phys. Chem.* **1981**, *85*, 1498.

(15) Chandrasekhar, J.; Jorgensen, W. L. *J. Chem. Phys.* **1982**, *77*, 5080.

(16) (a) Mezei, M.; Beveridge, D. L. *J. Chem. Phys.* **1981**, *74*, 6902. (b) Impey, R. W.; Madden, P. A.; McDonald, I. R. *J. Phys. Chem.* **1983**, *87*, 5071.

(17) (a) Clementi, E.; Barsotti, R. *Chem. Phys. Lett.* **1980**, *59*, 21. (b) Clementi, E.; Barsotti, R.; Fromm, J.; Watts, R. O. *Theor. Chim. Acta* **1976**, *43*, 101. (c) Fromm, J.; Clementi, E.; Watts, R. O. *J. Chem. Phys.* **1975**, *62*, 388. (d) Watts, R. O. *Mol. Phys.* **1976**, *32*, 659. See also ref 4c.

(18) (a) Heinzinger, K.; Vogel, P. C. *Z. Naturforsch., A* **1976**, *31A*, 463. (b) Vogel, P. C.; Heinzinger, K. *Ibid.* **1976**, *31*, 476. (c) Palinkas, G.; Riede, W. O.; Heinzinger, K. *Ibid.* **1977**, *32*, 1137. (d) Bopp, P.; Dietz, W.; Heinzinger, K. *Ibid.* **1979**, *34*, 1424. (e) Szasz, G. I.; Heinzinger, K. *Ibid.* **1979**, *84*, 840.

(19) Frank, H. S.; Wen, W.-Y. *Discuss. Faraday Soc.* **1957**, *24*, 133. Gurney, R. W. "Ionic Processes in Solution"; McGraw-Hill: New York, 1953.

(20) Neilson, G. W.; Page, D. I.; Howells, W. S. *J. Phys. D.* **1979**, *12*, 901. Neilson, G. W. *Chem. Phys. Lett.* **1979**, *68*, 247. Lee, Y. K.; Campbell, J. H.; Jonas, J. *J. Chem. Phys.* **1974**, *60*, 3537. Egelstaff, P. A.; Page, D. I.; Heard, C. H. T. *J. Phys. C* **1968**, *10*, 1793. See also ref 7.

(21) Smith, S. F.; Chandrasekhar, J.; Jorgensen, W. L. *J. Phys. Chem.* **1982**, *86*, 3308.

(22) Chandrasekhar, J., unpublished calculations. See also: Dierckson, G. H. F.; Kraemer, W. P. *Chem. Phys. Lett.* **1970**, *5*, 570. Dierckson, G. H. F.; Kraemer, W. P.; Roos, B. O. *Theor. Chim. Acta* **1975**, *36*, 249. Piela, L. *Chem. Phys. Lett.* **1973**, *19*, 134. Alagona, G.; Scrocco, E.; Tomasi, J. *Theor. Chim. Acta* **1978**, *47*, 133. Yamabe, S.; Ihira, N.; Hirao, K. *Chem. Phys. Lett.* **1982**, *92*, 172.

(23) Jorgensen, W. L.; Bigot, B.; Chandrasekhar, J. *J. Am. Chem. Soc.* **1982**, *104*, 4584.

single ion and 125 water molecules in a cube with periodic boundary conditions. Simulations for F^- and Cl^- with 216 water molecules were also carried out to check the size dependence of the results. The isothermal–isobaric (NPT) ensemble at 25 °C and 1 atm was employed in all cases.[24] In order to enhance the statistics for the solute and its near neighbors, a preferential sampling algorithm was used. In a modification of Owicki's scheme,[23,25] the probability of attempting to move a solvent molecule was made proportional to $1/(r^2 + C)$, where r is the distance between the ion and the oxygen atom of the water monomer. The constant C (50 Å^2) was chosen to make the number of attempted moves for the solvent molecules nearest the solute 3–4 times that for the farthest ones. The solute was also moved every 40th configuration to improve its sampling.

The initial configurations were generated from an earlier simulation on Na^+ in water.[15] For the simulations with 125 water molecules, equilibration was carried out over 1000K configurations and averaging was performed on the next 2000K configurations. New configurations were selected as usual by randomly translating the selected monomer or ion in the three Cartesian directions and for water by rotating randomly about a randomly chosen axis. Volume moves were made every 1000 configurations by scaling all the coordinates. The energy of the new configuration was computed from the pairwise sum over all of the interaction energies (eq 1) out to cutoff radii of 7.5 and 8.5 Å for the solutions with 125 and 216 water molecules, respectively. The acceptance of the new configuration was based on the Metropolis test with the necessary modifications for the preferential sampling.[25] The ranges for the moves were chosen to yield an acceptance rate of nearly 40%. Most of the calculations were performed on a Harris Corp. H-80 computer in our laboratory.

(c) Energy Component Analysis. The energy for the process of transferring the solute from the ideal gas phase into the solvent, ΔE_{sol}, can be obtained from simulations on the pure solvent and the dilute solution. The total energy of the solution is composed of the solute–solvent interaction energy, E_{SX}, and the solvent–solvent energy, E_{SS}. Denoting the energy of the pure solvent as E^*_{SS}, the energy of solution is given by

$$\Delta E_{sol} = E_{SX} + E_{SS} - E^*_{SS} = E_{SX} + \Delta E_{SS} \quad (2)$$

where ΔE_{SS} is the solvent reorganization energy.

It is possible to partition the solute–solvent energy and the solvent–solvent energy in the solution into components based on structural units defined by the solute–solvent radial distribution functions. Thus, the solvent molecules can be classified as belonging to the first solvation shell (region 1) or to the bulk (region 2), depending on the solute–solvent distance. The solute–solvent interaction energy, E_{SX}, can correspondingly be split into contributions arising exclusively from the first-shell solvent molecules, E_{SX1}, and from the bulk solvent molecules, E_{SX2}. Also, the solvent–solvent interaction energy, E_{SS}, can be divided into three components representing first shell–first shell (E_{11}), first shell–bulk (E_{12}), and bulk–bulk (E_{22}) interactions:

$$E_{11} = \sum_{i<j}^{\text{in 1}} \epsilon_{ij} \quad (3)$$

$$E_{12} = \sum_{i}^{\text{in 1}} \sum_{j}^{\text{in 2}} \epsilon_{ij} \quad (4)$$

$$E_{22} = \sum_{i<j}^{\text{in 2}} \epsilon_{ij} \quad (5)$$

In order to divide the solvent reorganization energy into components for the two regions, E_1 and E_2 may be defined as the contributions to E_{SS} arising from the n molecules in region 1 and from the $N - n$ molecules in region 2:

$$E_1 = E_{11} + E_{12}/2 \quad (6)$$

$$E_2 = E_{22} + E_{12}/2 \quad (7)$$

(24) McDonald, I. R. *Mol. Phys.* **1972**, *23*, 41.
(25) Owicki, J. C. *ACS Symp. Ser.* **1978**, *86*, 159.

Table II. Thermodynamic Results for Aqueous Ionic Solutions[a]

	Li^+	Na^+	F^-	Cl^-
E_{SX}	−231 ± 2	−195 ± 1	−212 ± 1	−143 ± 1
E_{SS}	−1190 ± 2	−1186 ± 2	−1155 ± 2	−1193 ± 3
E^*_{SS}	−1256 ± 2	−1256 ± 2	−1256 ± 2	−1256 ± 2
ΔE_{SS}	66 ± 4	70 ± 4	101 ± 4	63 ± 5
ΔE_{sol}	−165 ± 4	−125 ± 2	−111 ± 4	−80 ± 5
ΔH_{sol}	−165 ± 4	−126 ± 4	−111 ± 4	−80 ± 5
ΔH_{sol}(exptl)[b]	−130	−102	−116	−82
V	3651 ± 9	3684 ± 19	3795 ± 6	3791 ± 12
V^*	3748 ± 9	3748 ± 9	3748 ± 9	3748 ± 9
ΔV_{sol}	−97 ± 18	−64 ± 28	47 ± 15	43 ± 21
ΔV_{sol}(exptl)[c]	−11	−11	7	39

[a] All computed values are for one solute and 125 water monomers. Values for the pure solvent are indicated by an asterisk. Energies and enthalpies in kcal/mol; volumes in Å^3. [b] From ref 5. [c] From ref 28.

Clearly, E_{11} and E_{22} contribute exclusively to E_1 and E_2, respectively. Furthermore, E_{12} has conveniently been partitioned as making equal contributions to E_1 and E_2. The solvent reorganization energy associated with the first shell and the bulk can then be expressed as:

$$\Delta E_1 = E_{11} + E_{12}/2 - E^*_{SS}n/N \quad (8)$$

$$\Delta E_2 = E_{22} + E_{12}/2 - E^*_{SS}(N - n)/N \quad (9)$$

Thus, the total solvation energy, ΔE_{sol}, is now represented as the sum of the components given in eq 10.

$$\Delta E_{sol} = E_{SX1} + E_{SX2} + \Delta E_1 + \Delta E_2 \quad (10)$$

The definition of E_1 and E_2 (eq 6 and 7) based on the equal partitioning of E_{12} also means that $2E_1$ and $2E_2$ represent the total solvent–solvent interaction energies for first-shell or bulk molecules, respectively. The average solvent bonding energies per molecule for the first shell, E_S, and for the bulk solvent molecules, E_B, are then given by:

$$E_S = (2E_{11} + E_{12})/n \quad (11)$$

$$E_B = (2E_{22} + E_{12})/(N - n) \quad (12)$$

E_S and E_B have been used previously to interpret the hydrophobic hydration of apolar solutes.[14c,j,k] Although analyses of E_S and E_B can be valuable, ΔE_1 and ΔE_2 provide a more direct measure of the contributions to the solvent disruption in view of eq 10. Nevertheless, the components in eq 10 as well as E_S and E_B are reported for the various ionic solutions in the following.

In practice, the above analysis was performed on configurations saved at 5K intervals during the simulations. The minimum in the first peak in the ion–water oxygen radial distribution function was used as the cutoff radius for the first shell. The coordination number, n, and the components E_{SX1}, E_{11}, and E_{12} were then evaluated. Since the total values, E_{SX} and E_{SS}, were stored along with the coordinates, the remaining components E_{SX2} and E_{22} were obtained as the differences $E_{SX} - E_{SX1}$ and $E_{SS} - E_{11} - E_{12}$, respectively.

The energy decomposition procedure outlined above provides a general means for analyzing solutions. The analysis could be particularly valuable for investigating solutions with aprotic solvents for which a study of solvent reorganization via hydrogen bonding analyses is not possible. It must be emphasized that the above scheme is based on the assumption that the configurational energy can be written entirely in terms of two-body interactions.

Results and Discussion

(a) Thermodynamics. The calculated heats and volumes of solution are compared with experimental data in Table II. The reported uncertainties ($\pm\sigma$) for the computed quantities were obtained from separate averages over blocks of 50K configurations. It should also be noted that the experimental single ion heats of solution are Bockris' and Reddy's best estimates and require several assumptions in their derivation.[5] The uncertainties in these

numbers may be as much as ±10 kcal/mol.

An important issue in analyzing the results is the influence of system size on the computed quantities. The results in Table II do not include any cutoff corrections since there is no generally accepted procedure for making them. Mezei and Beveridge previously noted that the energetics of hydration for the ions varied by ca. 15% in going from 125 to 215 water molecules.[16a] Similar results were obtained in the present work for Cl^-; however, the heat of hydration for F^- showed a greater change. It was lowered from −111 to −146 kcal/mol in going from 125 to 216 water molecules. Perhaps surprisingly it is not a decrease in E_{SX} that is primarily responsible for the difference, but rather diminished solvent disruption in the larger system. Specifically, ΔE_{SS} for the F^- solution decreases from 101 to 69 kcal/mol, while E_{SX} is lowered by only 3 kcal/mol. It is apparent that significant edge effects exist in the solution for F^- with 125 water molecules. The edge effects are less for Cl^- and the cations and are much reduced for F^- in proceeding to 216 water molecules. This is evident in the ΔE_2 values discussed below whose magnitude also suggests that an increase in the system size beyond 125 water molecules for the cations and 216 for the anions should have relatively little effect on the thermodynamic results.

Following this analysis, it is clear that the present potential functions predict overly exothermic heats of solution for the ions with the largest error occurring for Li^+. The discrepancy is readily attributed to the lack of explicit three-body terms in the potential functions that are needed to account for the strong polarization of the first shell by the ions.[4,16-18] Nevertheless, the present potential functions are simpler and provide results at least as good as the prior alternatives[4] with significant improvement apparent for Cl^- and Na^+.[16]

The two principal components of the heat of solution, E_{SX} and ΔE_{SS}, are also given in Table II. The latter quantity is obtained from two simulations as the difference in the solvent–solvent energy in the solution and in the pure solvent. Consequently, its statistical uncertainty is greater than for E_{SX}. For the ionic solutions, the highly attractive E_{SX} is partially offset by the concomitant solvent disruption, ΔE_{SS}. For the solutes of like charge, it is found that the smaller ion has more attractive interactions with the solvent, but also causes greater solvent disruption. The same pattern is revealed in the results of Mezei and Beveridge,[16a] though their E_{SX} and ΔE_{sol} values are generally more exothermic than those obtained here.

The volumes of solution in Table II are also of interest and have not been computed previously. They are obtained readily in NPT simulations as the difference in the volumes for the pure solvent and solution. Though the statistical uncertainties in computing ΔV_{sol} are particularly large, the results can still be qualitatively useful as in revealing serious errors in the solute–solvent potential functions. In view of the lack of three-body terms and the overly exothermic heats of solution, the ionic solutions might be expected to show substantial contraction. The trend is apparent in the results for Li^+ and Na^+, but the effect is not severe in view of the statistical uncertainties and the total volumes of the systems. Some expansion is found for the F^- and Cl^- solutions with 125 solvent molecules; however, for 216 water molecules ΔV_{sol}'s of −55 ± 44 and −68 ± 63 Å^3 were obtained for these ions, respectively. The lessened edge effects and solvent disruption for the larger system size undoubtedly contribute to the reduced ΔV_{sol}'s. Overall, it appears that some extra contraction accompanies the too exothermic heats of solution for the ions, though gross errors are not evident.

(b) Solute–Solvent Structure and Energetics. The calculated ion–oxygen and ion–hydrogen radial distribution functions (rdf's) are shown in Figure 2. The ion–oxygen rdf's display two well-defined peaks in all cases. A similar pattern, but displaced to larger r, is found in the ion–hydrogen rdf's of the Li^+ and Na^+ solutions. In the aqueous solutions of F^- and Cl^-, one hydrogen atom of each first-shell water molecule is closer to the ion, resulting in the sharp first peak in the ion–hydrogen rdf's. The first maxima in the ion–oxygen rdf's for these two solutions occur nearly 1 Å farther away. The non-coordinating hydrogen atoms of the first-shell water molecules constitute the second peak in the ion–hydrogen rdf's. However, this feature merges into the contributions from the hydrogen atoms of water molecules in the second shell, particularly for the Cl^- solution. These results are qualitatively similar to those of Mezei and Beveridge[16a] and of Impey et al.[16b]

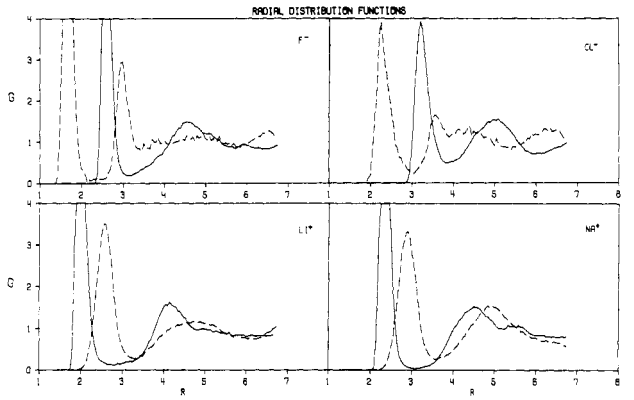

Figure 2. Computed ion–oxygen (solid lines) and ion–hydrogen (dashed lines) rdf's for Li^+, Na^+, F^-, and Cl^- in water. Distances in angstroms throughout.

Table III. Structural Results for the First Solvation Shell

	Li^+	Na^+	F^-	Cl^-
	Ion–Oxygen Distance (Å)			
this work	1.95	2.33	2.60	3.21
Clementi, MC[a]	1.95	2.33	2.5[b]	3.4[b]
Beveridge, MC[c]	2.10	2.35	2.60[b]	3.25[b]
Heinzinger, MD[d]	2.10	2.3	2.2	2.7
Impey, MD[e]	1.98	2.29	2.67	3.29
Clementi, for small clusters[f]	1.9–2.0	2.3–2.4	2.7–2.8	3.4–3.5
X-ray[g]	1.95–2.25	2.38, 2.4		3.10–3.35
neutron diffraction[h]	1.95			3.20–3.34
	Ion–Hydrogen Distance (Å)			
this work	2.60	2.90	1.65	2.25
Clementi, MC[a]	2.5[b]	3.0[b]	1.68	2.55
Beveridge, MC[c]	2.70[b]	2.90[b]	1.70	2.30
Heinzinger, MD[d]	2.6	2.8	1.2	1.7
Impey, MD[e]	2.57	2.95	1.73	2.35
neutron diffraction[h]	2.55			2.22–2.26
	Coordination Number[i]			
this work[j]	4.9 (10.6)	6.0 (13.2)	6.2 (6.2)	7.4 (7.0)
Clementi, MC[a]	5.0	5.4	5.0	5.6
Beveridge, MC[c]	5.97	5.96	4.09	8.36
Heinzinger, MD[d]	5.7	7.3	6.3	7.4
Impey, MD[e]	5.3	6.0	5.8	7.2
X-ray[g]	4–6	4, 6		5–11
neutron diffraction[h]	5.5			5.3–6.2

[a] Reference 17a. [b] Quoted in ref 7. [c] Reference 16a. [d] Reference 18. [e] Reference 16b. [f] Reference 4a. [g] Reference 7. [h] Reference 8. [i] See text for the different definitions used to obtain these values. [j] On the basis of ion–oxygen rdf's; values for ion–hydrogen rdf's in parentheses.

Experimental data on the solute–solvent structure in these solutions are essentially limited to the first solvation shell. In Table III, the positions of the first maximum in the ion–oxygen and ion–hydrogen rdf's obtained from various simulations are compared with available X-ray and neutron diffraction data.[7,8] There is generally good agreement between the calculated and experimental results, although there are occasional discrepancies in the earlier simulations. Thus, the distances involving the anions are too short in the MD studies of Heinzinger et al.,[18] while the Li–O distance of Mezei and Beveridge[16a] and the Cl–H distance of Clementi[17] are a little overestimated. The present results are uniformly good. Interestingly, the optimized bond lengths in small ion–molecule clusters using potential functions from Hartree–Fock calculations[3,4] agree well with the solution results (Table III). Rao and Berne have also noted that local solvation structures in aqueous

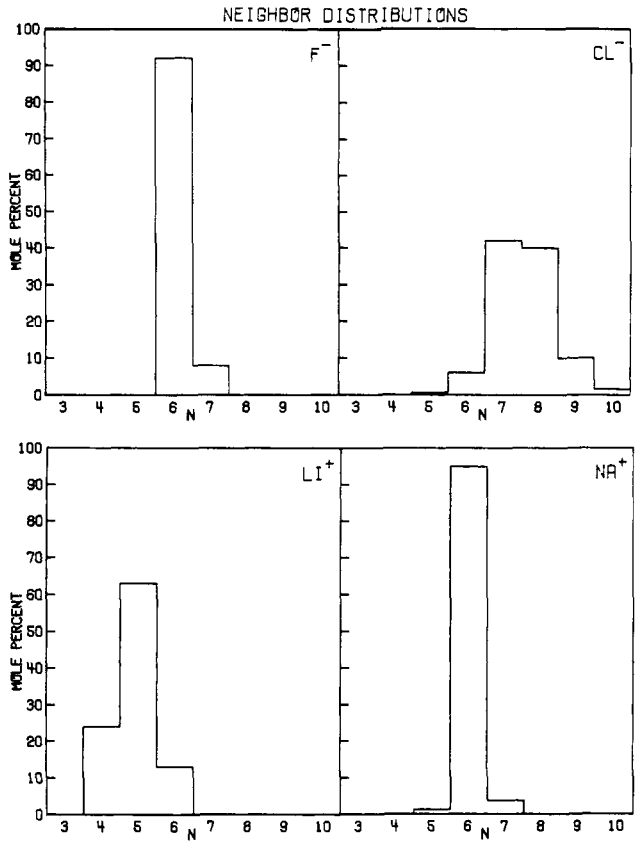

Figure 3. Computed distributions of coordination numbers for Li^+, Na^+, F^-, and Cl^- in water based on the first peak in the ion–oxygen rdf's.

ionic solutions are similar to those in relatively small clusters.[14]

The calculated coordination numbers for the ions are also compared with X-ray and neutron diffraction values in Table III. Both the calculated and the experimental values are sensitive to the definition of the coordination number. A wide range of experimental hydration numbers is available, for example, from mobility measurements.[5] These values correspond to the number of solvent molecules that have undergone some constant critical change due to the ion, a change which is susceptible to measurement by a particular experimental technique. Such hydration numbers are often quite different from coordination numbers based on a structural definition, like those from diffraction experiments.[7,8] Mezei and Beveridge obtained their values by integrating the ion–center of mass of water rdf's up to the minimum of the first peak.[16a] These values will not be significantly different if they are based on ion–oxygen rdf's instead. While this is a straightforward definition and has been adopted for all the calculated values for Li^+ and Na^+, alternative definitions are possible for Cl^- and F^- which participate in hydrogen bonds. For the present results, two sets of coordination numbers are reported on the basis of integration to the minimum after the first peak in the ion–oxygen as well as ion–hydrogen rdf's. For the cations, there are roughly twice as many hydrogens in the first peaks as oxygens consistent with the expected coordination to oxygen. However, for the anions the first peaks in the XH and XO rdf's contain essentially the same number of atoms. Consequently, hydration of the anions occurs through linear rather than bifurcated hydrogen bonds. The same geometry is preferred in the gas-phase ion–water clusters.[3,4,22] The calculated coordination numbers from the ion–oxygen rdf's compare favorably with experiment, taking into account the problems in the definition. In particular, the present results are close to the recent, accurate neutron diffraction studies on dilute aqueous solutions of Li^+ and Cl^-.[8]

The distributions of coordination numbers for the ions were also obtained from the simulations as shown in Figure 3. For the isoelectronic ions Na^+ and F^-, six-coordinate structures are the most common. The coordination number for Li^+ fluctuates in the range 4 to 6, while that for Cl^- extends from 6 to 10. These results are similar to the distributions obtained for Na^+ and Cl^- by Mezei and Beveridge.[16a] However, they found mostly five- and six-coordinate species, respectively, for the F^- and Li^+ solutions.

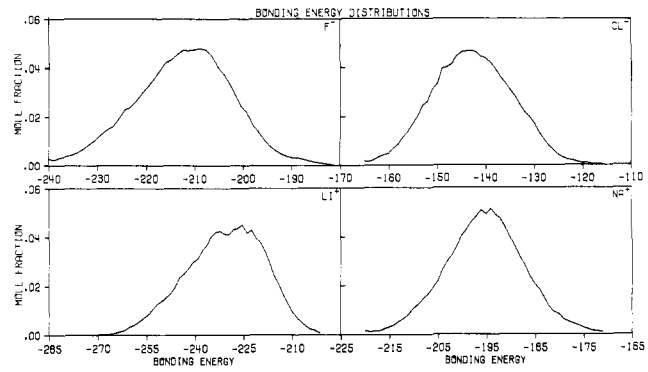

Figure 4. Computed solute–solvent bonding energy distributions for Li^+, Na^+, F^-, and Cl^- in water. The ordinate gives the mole fraction of solute with the bonding energy shown on the abscissa. Units for the ordinate are mole fraction per kcal/mol.

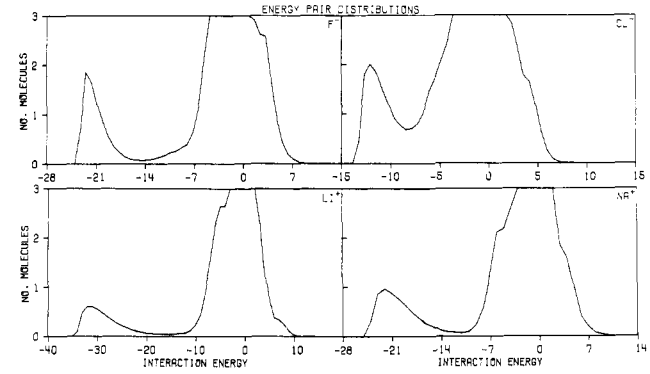

Figure 5. Computed solute–solvent energy pair distributions for Li^+, Na^+, F^-, and Cl^- in water. The plots record the number of solvent molecules bound to the ion with the energy given on the abscissa. Units for the ordinate are molecules per kcal/mol.

The varying tightness of the first shell in these systems is also reflected in the calculated rdf's. The minimum in the first peak of g_{Na-O} is nearly zero which indicates there is low probability for intermediate structures and consequently little exchange of first- and second-shell solvent molecules. The first peak in the Cl–O rdf, on the other hand, does not drop below 0.49, suggesting significant diffusion of water molecules occurs in and out of the first shell.

The range of total solute–solvent bonding energies in the solutions is shown in Figure 4. The distributions are all broad, spanning 50–60 kcal/mol. Only the plot for Li^+ is clearly polymodal; otherwise, the presence of differently coordinated ions cannot be discerned from these distributions. This is not surprising since the total bonding energies include ion–solvent interactions beyond the first shell as well.

The distributions of individual solute–solvent interaction energies are given in Figure 5. A well-defined peak corresponding to the interactions with the molecules in the first solvation shell is evident in each case. Integration of the peak yields coordination numbers of 4.8 for Li^+, 6.0 for Na^+, 6.2 for F^-, and 6.9 for Cl^-, similar to the values obtained from the ion–oxygen rdf's (Table III). The remainder of the distributions covers a wide energy range and represents the second shell and bulk solvent. Shoulders and inflexions in the attractive region probably correspond to ion–second solvent shell interactions. It may also be noted that the energetic distinction between the first shell and the rest of the solvent is much less pronounced for the Cl^- solution which is consistent with the distribution of coordination numbers (Figure 3). As discussed in an earlier study, significant repulsive ion–water interactions are also present in these solutions.[15] These occur

Table IV. Energy Components (kcal/mol) for Dilute Aqueous Solutions

	Li^+	Na^+	F^-	Cl^-	H_2O
E_{SX_1}	−138	−119	−129	−77	−16
E_{SX_2}	−92	−76	−83	−66	−6
E_{SX}	−231	−195	−212	−143	−22
$\langle E_{SX}\rangle^a$	−231	−195	−212	−143	−20
E_{11}	25	23	21	10	−3
E_{12}	−41	−57	−73	−96	−67
E^*_{12} [b]	−75	−91	−94	−111	−67
E_{22}	−1175	−1152	−1103	−1108	−1166
ΔE_1	54	55	47	36	8
ΔE_2	12	16	55	27	5
E_S	1.8	−1.8	−5.0	−10.4	−16.6
E_B	−19.9	−19.8	−19.2	−19.6	−20.1
n	4.9	6.0	6.2	7.3	4.4
$\langle n\rangle^a$	4.9	6.0	6.2	7.4	4.2
$E_{SX_1} + E_{11}$	−113	−96	−108	−67	−19
ΔH^{gas} [c]	−111	−97	− 80	−49	
cluster size[c]	5	6	5	4	

[a] Ensemble averages. [b] Calculated by assuming E_{12} to be proportional to n with the values for pure water as the reference. [c] Gas-phase enthalpy changes for the formation of ion-water clusters from ref 2a,b.

between the ion and the solvent molecules immediately surrounding the first shell which are engaged in establishing the hydrogen bonding network of water. Such repulsive ion–solvent interactions are not so significant in less extensively hydrogen bonded solvents like methanol and are practically absent in aprotic solvents like tetrahydrofuran.[15]

(c) Solvent Structure and Energetics. The calculated OO, OH, and HH rdf's in the solutions are virtually identical with those reported previously for the pure liquid.[11a] Although the formation of the first solvation shell represents a significant change in solvent structure, the number of molecules involved is small. The solvent disruption beyond the first shell is slight (vide infra), so the solvent–solvent rdf's are dominated by the bulk solvent contribution.

Solvent–solvent bonding energy and energy pair distributions also provide only limited information on solvent reorganization. Comparison of these results with those for the pure liquid indicates the presence of more repulsive solvent–solvent interactions in the solutions, presumably due to the interactions within the first shell. It is necessary to carry out more detailed structural and energetic analyses, as considered in the next section, to obtain a fuller understanding of the nature of solvent reorganization in these solutions.

(d) Energy Components. The computed values for the energy components defined in eq 3–12 are presented in Table IV. Besides the four ionic solutions, pure water was also analyzed as a dilute solution containing a water "solute".[29] The previous results with the TIP4P potential and 125 monomers were employed for this purpose.[11a]

In these calculations, the radius of the first shell is defined by the first minimum in the solute–water oxygen rdf's. Comparison of E_{SX}, ΔE_{sol}, E_{SS} ($=E_{11} + E_{12} + E_{22}$), and the coordination numbers obtained from the component analyses on the saved configurations with the corresponding complete ensemble averages provides a test for the numerical accuracy of the component calculations. The accord is seen to be excellent in Tables II and IV.

The interaction with the first shell, E_{SX_1}, is the largest contributor to the solute–solvent attraction; however, interaction with the bulk, E_{SX_2}, is substantial and accounts for 39–46% of E_{SX} for the ions. In addition, E_{SX_2} should decrease further with increasing system size, though, as noted above, E_{SX} is lowered only by 3–5 kcal/mol in going from 125 to 216 water molecules. Overall, the qualitative conclusion is that the ion–first shell and ion–bulk attractions are similar.

Of the three solvent–solvent energy components, E_{11} consists of interactions including only the first-shell molecules. In the reference system, pure water, the monomers in the first shell are hydrogen bonded to the water "solute". The interaction between these molecules amounts to a modest attractive energy, −3 kcal/mol. In comparison, the first shell–first shell interactions are significantly repulsive in the ionic solutions. This is not surprising, since the orientation of the first-shell molecules is mainly determined by the strong ion–water interactions. In fact, E_{11} parallels the gas-phase ion–water interaction energies (Table I); Cl^- has by far the weakest interaction with water and the smallest E_{11}. It constrains the first-shell water molecules less, which is also apparent in Figure 3, and consequently the water molecules are better able to optimize the water–water interactions.

The total interaction between the first shell and the bulk monomers, E_{12}, is uniformly attractive (Table IV). This is because E_{12} consists of $n(N-n)$ interactions, the most significant of which are the hydrogen bonds linking the first shell to the bulk. If the interfacial hydrogen bonding is similarly efficient in all the solutions, E_{12} should be approximately proportional to the coordination number, n. The calculated E_{12} values do follow the trend in the number of molecules in the first shell, with the exception of the water "solution". Since the interfacing of the first shell with the bulk is perfect in pure water, the corresponding E_{12} and n can be used in conjunction with the ion coordination numbers to derive a set of idealized first shell–bulk interaction energies, E^*_{12} (Table IV). Comparison of E^*_{12} with E_{12} indicates significant disruption in the first shell–bulk interaction in the ionic solutions. The disruption is a direct consequence of the orientational constraints imposed by the ion on the first-shell monomers, rendering their interaction with the bulk to be less than optimal. Among the solutions, the first shells for the cations appear to be held more rigidly as indicated by the larger $E_{12} - E^*_{12}$ difference, 34 kcal/mol, for Li^+ and Na^+, compared to 21 and 15 kcal/mol for the solutions of F^- and Cl^-.

E_{22} represents the numerous bulk–bulk interactions, so it is correspondingly large and negative for all the solutions (Table IV). Although the calculated values show considerable variation, they must be interpreted with care due to the variation in coordination numbers. Thus, it appears that the bulk interactions in the anionic solutions are less attractive; however, this is partly due to the higher coordination numbers which lower the number of interactions contributing to E_{22}.

The results for E_{11}, E_{12}, and E_{22} have been used to partition the solvent reorganization energy, ΔE_{SS}, into two components, ΔE_1 and ΔE_2, corresponding to the disruption for the first shell and the bulk (eq 8 and 9). In Table IV, the positive ΔE_1 values show that the formation of the first shell causes significant loss of solvent–solvent attraction in all solutions. Interestingly, ΔE_1 is nearly the same for Li^+ and Na^+ in spite of their differing coordination numbers. This reorganization term is less for the anions, particularly for the Cl^- solution. Disruption also occurs beyond the first shell, though for the cations it only amounts to 12–16 kcal/mol. For the anions, the figures are larger, but this may be attributed in part to the edge effects discussed above. The results with 216 water molecules show that the solvent disruption for F^- and Cl^- is reduced by 32 and 9 kcal/mol, respectively, which should lower the ΔE_2 values for the anions to around 20 kcal/mol. It is important to remember that the ΔE_2 values also contain half of the interfacial disruption that is given roughly by the difference between E_{12} and E^*_{12}. Consequently, the key finding is that the solvent disruption occurs primarily within the first shell and in the interface between the molecules in the first shell and the remainder of the solvent.

The conclusions based on ΔE_1 and ΔE_2 are reinforced by the solvent bonding energy per molecule calculated for the first shell, E_S, and bulk, E_B. Compared to water molecules in pure water, the first-shell molecules in the ionic solutions have much less favorable interactions with the solvent. In fact, E_S is repulsive

(26) Jorgensen, W. L. *Chem. Phys. Lett.* **1982**, *92*, 405.
(27) Reviews: Millero, F. J. *Chem. Rev.* **1971**, *71*, 147. Horne, R. A., Ed. "Water and Aqueous Solutions"; Wiley-Interscience: New York, 1972; p 513.
(28) Kawaizumi, F.; Zana, R. *J. Phys. Chem.* **1974**, *78*, 627. Zana, R.; Yeager, E. B. *Ibid.* **1966**, *70*, 954; **1967**, *71*, 521, 4241.
(29) Hirata, F.; Rossky, P. J. *J. Chem. Phys.* **1981**, *74*, 5324.

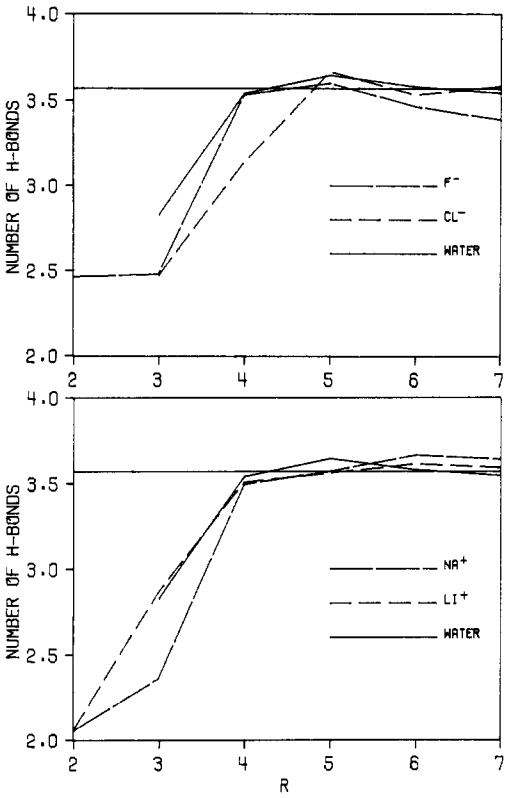

Figure 6. The average number of hydrogen bonds for each solvent molecule as a function of distance from the ion in the solutions of Li^+, Na^+, F^-, and Cl^- in water. Results for the aqueous "solution" of water are also indicated. The horizontal line corresponds to the average number of hydrogen bonds calculated for monomers in pure water.

for the Li^+ solution. E_S becomes more attractive in the halide solutions, particularly for Cl^-. The bulk monomers in the solutions also have a smaller bonding energy per molecule than those in the pure solvent due to the interfacial disruption and edge effects for the anions. Although the differences in E_B are small, the large number of bulk monomers causes their cumulative effect to yield the significantly repulsive ΔE_2 values since $\Delta E_2 = (N - n)(NE_B - 2E^*_{SS})/2N$. It should also be noted that the less negative E_S than E_B for pure water results from neglecting the interaction with the "solute" in computing E_S.

(e) Hydrogen Bonding Analyses. In order to obtain additional information on the structure of the solutions, the hydrogen bonding for the solvent molecules was also analyzed. As in the past, an energetic definition of hydrogen bonding was adopted. Specifically, any pair of solvent molecules bound by 2.25 kcal/mol or more is considered hydrogen bonded.[11,15] This cutoff roughly coincides with the minimum in the energy-pair distribution for pure water.[11]

An important distribution, shown in Figure 6, is for the number of solvent–solvent hydrogen bonds per monomer as a function of distance from the solute. The analyses were made on shells 1 Å thick and the horizontal line in the plots indicates the average number of hydrogen bonds (3.6) for pure water. Figure 6 also includes the results of the same analysis for pure water. Again, any hydrogen bond to the "solute" was not counted.

In water "solution", the presence of the "solute" reduces the number of solvent–solvent hydrogen bonds for the first-shell region by one. However, the average number quickly reaches the bulk value within 4 Å of the solute. A qualitatively similar situation is found in all the ionic solutions. The number of solvent–solvent hydrogen bonds in the vicinity of the ion is much less than the bulk value, but the bulk value is rapidly reestablished within 4–5 Å of the ion, i.e., in the second-shell region. The disruption of hydrogen bonding near the ion is greater in the solutions of Li^+ and Na^+. In these solutions, the water monomers in the first shell form only two hydrogen bonds per monomer. The corresponding values in the anionic solutions are higher by nearly 0.5.

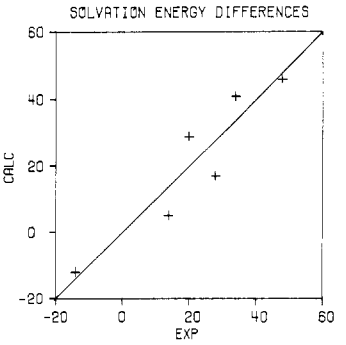

Figure 7. The calculated differences in the energy of formation of the first shell, ΔE_{fs}, vs. differences in the experimental heats of solution for pairs of ions including Li^+, Na^+, F^-, and Cl^-. All energies are in kcal/mol.

Beyond 5 Å the number of hydrogen bonds stays close to the bulk value in each case except for F^- which reveals some tailing off. This is consistent with the notion that for 125 water molecules, edge effects are only substantial for the F^- solution, as discussed above. Furthermore, it is apparent that none of the ions could be called structure makers, if this concept implies a pronounced increase in solvent–solvent hydrogen bonding.

(f) First-Shell and Gas-Phase Clusters. The sum of E_{SX1} and E_{11} is the energy associated with the first solvation shell, E_{fs}. These values are compared with gas-phase cluster-formation enthalpies, ΔH_n^{gas}, for the ions in Table IV.[1,2a,b] The cluster size n used in the comparisons is the nearest integral value of the coordination number for Li^+ and Na^+ (5 and 6, respectively). The gas-phase and solution energies are remarkably close for these two ions. For the anions F^- and Cl^-, clustering energies are available only up to sizes of 5 and 4, respectively, which are less than the solution coordination numbers based on ion–oxygen rdf's. Therefore, the solution energies are more negative. These results along with the earlier comparison of ion–water bond lengths (Table III) suggest that the gas-phase clusters are structurally and energetically similar to the ions plus first solvation shells found in solutions, if the cluster size is the same as the coordination number in solution.

The energy of the first shell, E_{fs}, has an added significance: the calculated values are similar in magnitude to the total heats of solution and also correctly reproduce their trends (Tables II and IV). Consequently, the differences in E_{fs} and in the experimental enthalpies of solution are similar, as shown for the six pairs of ions treated here in Figure 7. This result is in striking contrast to the earlier discussion on gas-phase clustering energies, which did not always reproduce the trends in total heats of solution (Figure 1). It is now easy to predict when the gas-phase results will be successful in this regard. Cluster-formation energies yield the correct solution trends only when the number of solvent molecules in the cluster is at least as high as the coordination number in solution. Second, differences in ΔH_n^{gas} for the same n will not necessarily be equal to the differential solvation energies if the coordination numbers of the ions considered are significantly different in solution. As indicated by Figure 7 and Table IV, use of ΔH_n^{gas} values for complete first-shell clusters will be more accurate. Unfortunately, reliable solution coordination numbers are not often available to interpret gas-phase results. The converse of the present conclusions could then be valuable. If the ΔH_n^{gas} values are close to the total heats of solution, the clusters may be assumed to be at least as large as the first solvation shell found in solution. If the differential solvation energies from the clusters do not parallel the differences in heats of solution, the clusters are too small and/or the solution coordination numbers for the solutes considered are significantly different.

The observations concerning E_{fs} made here are empirical and warrant further investigation. In particular, they imply that $E_{SX2} + E_{12} + E_{22}$ may be approximately constant for different ionic solutions even with different coordination numbers. If this is generally valid, it would be most useful for further development of solution theories.

Conclusions

The simple ion–water potential functions reported here when used in conjunction with the TIP4P potential for water were demonstrated to provide reasonable descriptions of dilute aqueous solutions of Li^+, Na^+, F^-, and Cl^-. The computed heats of solution showed improvement over previous work, and the structural results are in excellent accord with available diffraction data. The average coordination numbers for Li^+ and Na^+ are 5 and 6, while F^- and Cl^- participate in an average of 6 and 7 linear hydrogen bonds, respectively. Furthermore, the weaker ion–solvent interactions for Cl^- lead to a more flexible first shell exhibiting the broadest range of coordination numbers (6–10).

A scheme for decomposing the computed energetics of the solvation process was provided and led to several observations. (1) The orienting influence of the ions is clearly apparent in the net repulsive solvent–solvent interactions that are found between water molecules in the first shell. (2) The total ion–solvent attraction is about evenly divided between the first shell and the remainder of the solvent. (3) The solvent disruption is localized in the first shell and in the interface to the first shell. This point was supported by hydrogen bonding analyses which revealed that water molecules beyond only 4–5 Å from the ions participate in normal numbers of hydrogen bonds.

The definition of the energy components also permitted comparisons of results for the solutions and gas-phase ion–water clusters. It was found that the energetics associated only with the first solvent shell ($E_{SX1} + E_{11}$) are enough to determine the trends in total heats of solution for the ions. Moreover, the ions plus their first solvation shells are structurally and energetically similar to ion–molecule clusters in the gas phase, if the coordination numbers match the cluster size. These observations provide important links between gas-phase and solution chemistry.

Acknowledgment. Gratitude is expressed to the National Science Foundation (CHE80-20466) for support of this work.

Thermodynamics of Solution of Naphthalene in Various Water–Ethanol Mixtures‡

Donald Bennett and William J. Canady*

Contribution from the Department of Biochemistry, West Virginia University Medical Center, Morgantown, West Virginia 26506. *Received February 24, 1983*

Abstract: The temperature dependences of the solubilities of naphthalene in water and in various water–ethanol mixtures up to 0.07 mol fraction of ethanol have been determined. In the concentration range studied, a plot of the free energy of solution of naphthalene vs. mole fraction of ethanol present in the solvent is linear. The heat of solution of naphthalene in water is positive and becomes more positive as the ethanol concentration is increased. This heat term is more than overcome by a concomitant large increase in the entropy of solution, the net effect being to solubilize the hydrocarbon by the addition of ethanol. The addition of ethanol to the aqueous phase is much more effective in solubilizing naphthalene at high rather than at low temperatures. The results may be interpreted in terms of the McMillan–Mayer second virial coefficient. It is suggested that ethanol may exert its influence upon hydrocarbon solubility by loss of water structure as hydrophobic interactions take place between the hydrocarbon and alcohol. Dispersal of an iceberg or clathrate structure probably makes a significant contribution.

Introduction

The solubility of naphthalene in mixed organic solvents has been of interest to the present authors because, by making some reasonable simplifying assumptions, it is possible to relate the variation of solubility of a substrate such as naphthalene to the ability of the enzyme(s) cytochrome P-450 to bind it.[1] Since the solubility of naphthalene was found to vary in an interesting manner with variations in composition of water–ethanol solvent mixtures at a single temperature and since there appears to be very little data available on the effects of addition of organic solvents upon the aqueous solubility of hydrocarbons, it was deemed advisable to study the temperature dependence of the solution process in order to ascertain the effects of added organic solvent (ethanol) upon the thermodynamics of solution for naphthalene. Such a study might shed some light upon the process of solubilization of a simple but fairly bulky aromatic hydrophobic compound by the addition of an organic solvent to the aqueous medium. In addition, the use of a crystalline solid tends to minimize the effects of extraction of ethanol from the aqueous medium by a liquid hydrocarbon were such a compound chosen for the study.

The purpose of the present work is to determine the dependence of the thermodynamics of solution of naphthalene in solvent mixtures ranging from pure water to a water–ethanol mixture containing 0.07 mol fraction of ethanol. In this range, it has been found that the free energy of solution varies in a linear manner with the mol fraction of ethanol present in the ethanol–water solvent. At higher ethanol concentrations than this, a different law applies to the solubilities and will be considered at a later time.

Experimental Section

Materials and Methods. The naphthalene was obtained from the Fisher Scientific Co. and was zone-refined. In addition, it was recrystallized from 95% ethanol before use (mp 80–81 °C). The water–ethanol solutions were prepared from double-glass-distilled water and absolute ethanol (USP) obtained from U.S. Industrial Chemicals Co., New York, NY, and used without further treatment.

Naphthalene (0.2 g) was weighed out and rapidly added to 100 mL of water or water–ethanol mixture in a Virtis homogenizer flask which had been sealed and allowed to equilibrate at the working temperature for 30 min. The Teflon cover was attached and adjusted for best seal. The solution was stirred at approximately 25 000 rpm for a total of 2 min with a Virtis Model 23 homogenizer. Actually, no material increase in solubility could be demonstrated by increasing the stirring time beyond 1 min. The other details of the experimental techniques, equipment, temperature control, and measurement have been previously described.[2,3] The sintered glass tube used for sampling (previously equilibrated at working temperature; see ref 3) was rinsed with the naphthalene solution

‡Supported by the Department of Energy/Morgantown Energy Research Center, Contract DY-77-C-21-8087, and the West Virginia Medical Corporation.

(1) W. L. Backes and W. J. Canady, *Pharmacol. Ther.* **12**, 133 (1981).
(2) R. J. Larese and W. J. Canady, *J. Phys. Chem.*, **65**, 1240 (1961).
(3) R. J. Larese, D. A. Robinson, W. F. Brassine, and W. J. Canady, *J. Phys. Chem.*, **66**, 897 (1962).

0002-7863/84/1506-0910$01.50/0